Solid Dispersions of Carvedilol with Porous Silica

Borut Kovačič,[a,b] Franc Vrečer,[a,b] and Odon Planinšek*,[b]

[a] *Krka d. d.; Šmarješka cesta 6, 8501 Novo mesto, Slovenia: and* [b] *Faculty of Pharmacy, University of Ljubljana; Aškerčeva 7, 1000 Ljubljana, Slovenia.*

Received June 15, 2010; accepted January 17, 2011; published online January 17, 2011

Solid dispersion particles of carvedilol (CAR) were prepared with porous silica (Sylysia 350) by the solvent evaporation method in a vacuum evaporator to ensure an effective pore-filling procedure. Two sets were prepared, each with various amounts of CAR in solid dispersions, and with the pore-filling process differing each time. Set A was prepared by a one-step filling method and set B by a multiple-step pore-filling method of CAR into porous silica. The solid dispersions were then characterized using thermal analysis, X-ray diffraction, and nitrogen adsorption experiments. The results showed that the drug release can be significantly improved compared with the dissolution of the drug in its pure crystalline or amorphous state. Drug release from solid dispersion was faster when the drug content in the solid dispersion was low, which enabled the drug to be finely dispersed along the hydrophilic carrier's surface. The results also showed that a multiple-step pore-filling procedure is more effective for drug loading as indicated by the absence of a crystalline drug state, greatly reduced porosity, and improved wettability and physical stability of the amorphous CAR.

Key words carvedilol; porous silica; solid dispersion; dissolution rate improvement

Many newly developed active pharmaceutical ingredients exhibit low oral bioavailability due to their poor aqueous solubility and pre-systemic metabolism. This creates recognized difficulties in developing new pharmaceutical products.[1)] For drugs in class II and some in class IV of the Biopharmaceutics Classification System,[2)] the dissolution rate is what limits the drug absorption rate. Carvedilol (CAR), an arylethanolamine type α_1-receptor and β-adrenoceptor blocker used for patients with hypertension and congestive cardiac failure, is a drug that has a low level of solubility in gastrointestinal fluids and is extensively metabolized in the liver.[3)]

Increasing CAR's solubility can improve its bioavailability up to fourfold.[4)] One way to improve the dissolution rate is as describes Noyes–Whitney equation[5)] to increase the total surface area using micronization to reduce the particle size.[6)] Alternatively, the dissolution rate of CAR can be improved effectively by increasing its solubility through formation of the cyclodextrin inclusion complex[7—9)] or through the preparation of self-emulsifying drug delivery systems (SEDDS) or self-microemulsifying drug delivery systems (SMEDDS).[4)] The disadvantages of these methods are the complexity of their preparation and the necessity of using expensive excipients.

Another method of improving the dissolution rate of a drug is through amorphization and stabilization of its amorphous compounds in the drug product.[10,11)] The amorphous form of a drug usually has an improved dissolution rate compared to the crystalline form, but it is rarely used in pharmaceutical preparations due to its hygroscopicity and tendency towards crystallization.[12,13)] Common techniques for producing an amorphous state are the quench-cooling of a melt, dehydration, freeze drying, spray drying, and grinding.[14)] In addition to these methods, the preparation of a solid dispersion is a useful method for dispersing drugs in their molecular state into a matrix carrier such as povidone (PVP)[15)] or polyethylene glycol (PEG).[16)] Pokharkar *et al.*[17)] investigated the solid dispersion properties of CAR, PVP, and nonporous silica and found that such solid dispersions allowed for higher dissolution rates and the improved stability of amorphous CAR against crystallization. The stability improvement, however, was attributed to PVP, which caused an elevation in the amorphous form's glass transition temperature (T_g) value, hydrogen bonding, entrapment of drug molecules in the polymer matrix, and surface adsorption of amorphous silica.

Adsorption onto silica-based high-surface-area carriers is a known method of drug dissolution rate improvement that was first described in the early 1970s.[18)] Rigorous studies of drug dissolution rate improvement were performed by Rupprecht *et al.*[19)] and Vrečer.[20)] Recently, some authors have described the preparation of solid dispersions with porous silica, prepared by spray-drying,[21)] melt grinding,[22)] or the solvent method.[23)] Porous silica (Sylysia) contains many silanol groups on its surface and can be used as a pharmaceutical excipient, because it is regarded as nontoxic for oral consumption.[24,25)] Due to its porous structure and large specific surface area, porous silica's capacity to adsorb organic compounds is high. Such preparations influence the drug release rate and improve the amorphous drug's stability.[19—23)] Porous silica can be exploited for improving flow properties of dry powders[26)] and Takeuchi *et al.*[27)] reported that tablet-pressing process and tablet properties were also improved when drug substance (indomethacin) was included in solid dispersion with porous silica (Sylysia 350) in comparison to a physical mixture. This proves that the preparation of drug-porous silica solid dispersion is a very promising method also for pharmaceutical production of tablets or capsules.

Various methods are described for incorporating a drug into the porous silica matrix during its synthesis. One of them is known as the sol–gel process. It involves preparation of a colloidal suspension (sol) from an organic silicate followed by chemically-induced gelation (wet gel) and drying (dry gel state or xerogel).[28)] During the process, drug molecules may be present in the colloidal suspension of silica and are loaded into the porous network.[29)] Alternatively, porous silica gel can be stirred into a drug solution or suspension for a longer period of time, followed by rinsing the non-entrapped drug and then drying.[30)] The substantial loss of drug during such a preparation procedure can be prevented by

* To whom correspondence should be addressed. e-mail: odon.planinsek@ffa.uni-lj.si

using a minimal amount of solution to aid in complete sorption. The pore filling can be improved through repetition of the filling procedure several times. It is possible to achieve content of 500 mg of the active pharmaceutical ingredient in 1 g of the carrier.[31] High drug content can also be achieved by immersing porous silica gel in the drug solution and then evaporating the solvent using the spray-drying process or under reduced pressure.[19,32]

The purpose of this study was to prepare solid dispersion of CAR with porous silica and to compare different materials (porous and nonporous silica) and preparation methods (one step filling, multiple step filling) in terms of pharmaceutical performance (improved dissolution rate and physical stability) of active ingredient. To get insight into deposition mechanism of drug molecules into porous structure and explanations for different dissolution properties and stability of amorphous drug, which is incorporated within porous matrix relevant physicochemical properties were measured. Solid dispersion particles of CAR with porous silica (Sylysia 350) and nonporous hydrophilic silica (Aerosil 200) were prepared using the solvent evaporation method. Various evaporating procedures and drug-to-silica ratios, were used to prepare samples of solid dispersions. Changes to the crystalline state of CAR in solid dispersions were investigated using differential scanning calorimetry (DSC) and X-ray powder diffractometry (XRPD). The solid dispersions were also examined using scanning electron microscopy (SEM), specific surface area, and wetting measurements as well as a determination of particle size and CAR's dissolution behavior. After 12 months, the crystallization of amorphous CAR in solid dispersions was evaluated. Liquid dispersions of dissolved CAR and undissolved porous (Sylysia 350) and nonporous hydrophilic (Aerosil 200) silica were also prepared to measure the adsorption capacity of CAR on the silica surface.

Materials CAR (1-(9*H*-carbazol-4-yloxy)-3-[2-(2-methoxyphenoxy)ethylamino]propan-2-ol) was supplied by Krka d. d., Novo mesto (Slovenia). CAR is practically insoluble in water, mildly soluble in alcohol (ethanol 96%), soluble in methanol and tetrahydrofuran (THF). Upon crystallization of CAR from the THF solution, polymorph form II was obtained with the same DSC, X-ray, and Fourier transform (FT)-IR characteristics as the supplied ingredient.

Silica gel (Sylysia 350, Fuji Silysia Chemical Ltd., Japan) was used as a carrier in solid dispersion particles. Sylysia 350 is a porous hydrophilic excipient with GRAS (Generally Recognized as Safe) status.[26] An average particle size ranges from 3.1 to 20.0 μm, with a total pore volume between 1.25 and 1.60 ml/g and specific surface area of around 280 m^2/g.

Nonporous hydrophilic silica (Aerosil 200, Evonik-Degussa, Germany) was used for the adsorption studies and as a carrier in alternative solid dispersion particles. Its average specific surface area is 200±25 m^2/g.

Tetrahydrofuran (THF), methanol, and other chemicals were of reagent grade and were used as received. Water was purified by reverse osmosis.

Experimental

Preparation of Amorphous CAR Pure amorphous CAR was prepared by melting the crystalline substance over a paraffin oil bath that was maintained at 130 °C, slightly above the melting temperature. The melted drug was solidified by cooling it in a freezer. The purity of the obtained sample was checked using HPLC. Grinding of the amorphous CAR to the desired particle size was performed with vibrational micro mill Pulverisette 0 (Fritsch, Germany) for 5 min. Mortar, milling ball and closing lid was cooled in refrigerator (−18 °C) for 1 h before operation.

Table 1. Prepared Samples of SD and Their CAR Content

Sample	CAR (g)	Sylysia (g)	CAR content in SD (%)
Set A			
C0.5	0.5	2.0	20
C1	1.0	2.0	33
C2	2.0	2.0	50
C4	4.0	2.0	67
C6	6.0	2.0	75
Set B			
C2×0.5	2×0.5	2.0	33
C4×0.5	4×0.5	2.0	50
C6×0.5	6×0.5	2.0	60

Preparation of SD Particles The solid dispersion (SD) particles of CAR with porous silica particles were prepared using the solvent evaporation method. Two sets of samples were prepared:

Set A: Amount ranging between 0.5 g and 6.0 g (1.2—14.8 mmol) of CAR was dissolved in 20 ml of THF, as listed in Table 1. In the prepared drug solution, 2.0 g of porous silica was suspended for a few minutes and the suspension was evaporated by a rotary evaporator (IKA RV 05, Staufen, Germany) at a temperature of 50 °C with pressure values ranging from 70 to 130 mbar.

Set B: 0.5 g of CAR was dissolved in 20 ml of THF. In the prepared solution, 2.0 g of porous silica was suspended and the suspension was evaporated by a rotary evaporator at a temperature of 50 °C with pressure ranging from 70 to 130 mbar. When the solvent appeared to be evaporated, the pressure in the rotary evaporator was decreased to 50 mbar for 1 h to remove the THF. Then, another solution of 0.5 g CAR in 20 ml THF was prepared and added into the same flask with the prepared dry particles of 0.5 g CAR and 2.0 g silica. After a few minutes, the suspension was evaporated and dried as before. This loading step was performed 2, 4, and 6 times. Theoretical content values of CAR in SD particles are listed in Table 1, determined content values of CAR in SD particles deviated within range ±5% from theoretical values.

Permitted daily exposure of THF in pharmaceutical product is 7.2 mg and is regarded as "solvent to be limited."[33] Therefore the prepared samples of set A and set B were additionally dried in a vacuum chamber (Heraeus, Germany) at room temperature for 1 h to remove the remaining THF.

Samples were stored in a desiccator until further analysis. After the initial analysis at time zero, some of the samples were stored in a high-density polyethylene (HDPE) container for 12 months at ambient conditions (20—25 °C, 60—80% relative humidity (RH)).

Following the same procedure, solid dispersions of CAR with nonporous silica particles were prepared (Aerosil 200) that had a drug-to-silica ratio of 1 : 1 (2.0 g CAR, 2.0 g Aerosil 200, 20 ml THF; sample C2Ae). In order to study silica's adsorption capacity for CAR from the THF solution onto the silica surface, 2.0 g of CAR was dissolved in six 50 ml aliquots of THF. Then 0.00 g (control), 0.33 g, 0.50 g, 1.00 g, 2.00 g, and 4.00 g of silica (Aerosil 200 and Sylysia 350) were dispersed into the solution respectively. The prepared liquid dispersions matched the same quantitative proportions of CAR and silica as the prepared SDs of set A. The dispersion was gently stirred for 48 h and then ultra-centrifuged. Afterwards, the drug content in the supernatant was determined.

Product Characterization. Particle Size Determination The size of the drug and solid dispersion particles was measured using a Mastersizer S laser diffractometer (Malvern Instruments, Worcestershire, U.K.) equipped with a small sample dispersion unit that was diluted with water and a small amount of detergent (Tween 80, concentration 1.0 μg/ml) to improve the particles' dispersion rate. Laser diffraction measures the volume-based diameter distribution in the size range of 0.05 to 1000 μm.

Differential Scanning Calorimetry (DSC) and Thermogravimetric Analysis (TGA) DSC and TGA examinations were carried out using Mettler Toledo DSC and TGA instruments (Columbus, OH, U.S.A.), which were calibrated by the indium standard. The samples for DSC examination were placed in non-hermetically sealed aluminum pans and heated from −10 to 130 °C at a rate of 20 °C/min and given a nitrogen purge of 20 ml/min. The samples for TGA examination were placed in Sapphire discs and heated

from 30 to 200 °C. The output was evaluated by STARe 9.10 software.

X-Ray Diffractometry X-Ray diffractograms were obtained using a Philips PW3040/60 X'Pert PRO diffractometer (Philips Electronic Instruments, Mahwah, NJ, U.S.A.) using CuK_0 radiation (l=1.5418 Å) at 40 kV and 30 mA. Data was collected from 2 to 70° at 0.04° increments.

Specific Surface Area and Porosity Parameters Specific surface area and porosity parameters were determined using the Brunauer–Emmet–Teller (BET) technique based on nitrogen gas adsorption (Micromeritics Tristar 3000, Norcross, GA, U.S.A.) with relative pressure intervals from 0.05 to 0.3.[34] The total pore volume was estimated using the *t*-plot method of Lippens and De Boer.[35] The pore-size distribution was derived from the adsorption branches of the nitrogen isotherms using the BJH model.[36] Prior to this, 200-mg samples were slowly outgassed.

Scanning Electron Microscopy (SEM) The morphology of CAR, Sylysia, and the SD was analyzed using SEM. Dried samples were pressed on double-sided adhesive carbon tape (SPI Supplies, U.S.A.). Then the samples were imaged using a field emission scanning electron microscope (FE-SEM, Supra 35 VP, Carl Zeiss, Germany).

Wetting Properties Wetting properties of the drug and prepared SD were examined using Drop Shape Analysis (Krüss, Germany). Two hundred milligrams of the sample was pressed into round plates (diameter 1.2 cm) with a force of 2000 kg. A 2 μl drop of dissolution media (phosphate buffer solution pH 6.8) was placed on the surface of the pressed sample. Wetting properties were determined by observing the volume of the drop as it "disappeared" into the porous structure due to imbibition. Drop imbibition was analyzed using the Drop Shape Analysis program for Windows, v 1.90.0.14. Wetting dynamics were expressed as a function of drop volume *vs.* time and the slope of the function [μl/s] corresponds to the rate of imbibition. A faster rate of imbibition of liquid is a characteristic of better wettability and/or greater porosity. Wettability was also characterized by the static contact angle of liquid on the surface[37] and was determined with samples where imbibition did not occur. While analyzing the porous substrates, the contact angle was estimated at a time near zero (0—80 ms after drop placement), just as the drop had spread out completely and before imbibition took place to any greater extent.

Determination of Drug Content The drug content of the SD samples was determined by suspending approximately 30 mg of solid dispersion in a suitable quantity of methanol. It was checked and confirmed by preliminary tests that a time span of 2 h was sufficient to remove the entire drug load from the silica pores. Quantification of the drug in the filtered solution was determined using a UV-spectrophotometer (Agilent 8453, Germany) at a wavelength of 243 nm with a quartz cell, which had an optical path of 10 mm. The CAR content in the SD was also confirmed using a Perkin Elmer CHN analyzer. The standards used to construct the calibration curves were prepared using the same media. All analyses were performed in triplicate, and the mean values obtained from these experiments were used to calculate the maximum drug release in the *in-vitro* dissolution experiments.

Dissolution Study The dissolution studies were performed using a USP type II apparatus (VK 7000, VanKel, Cary, NC, U.S.A.), equipped with standard glass vessels and paddles. Samples equivalent to 25 mg of CAR (the maximum single dose) were placed in a dissolution vessel that contained 900 ml of phosphate buffer solution (pH 6.8) then maintained at 37±0.5 °C and stirred at 50 rpm. All the dissolution experiments were carried out in triplicate. Samples were collected periodically, filtered through a 0.45 μm pore filter (Minisart RC 25, Sartorius, Göttingen, Germany) and replaced with a fresh dissolution medium. The concentration of CAR was determined spectrophotometrically at 243 nm using UV-spectrophotometer.

Results and Discussion

Characterization of Amorphous and Crystalline CAR The amorphicity of quench-cooled CAR was determined using DSC and X-ray measurements (Figs. 1A, B). The DSC curve of crystalline CAR showed an endothermic peak at 115 °C, dH=−128 J/g, a characteristic of the melting of form II.[38,39] The DSC curve of amorphous CAR did not show the melting transition, but a T_g appeared at 38 °C. The XRPD of crystalline CAR showed characteristic peaks in the range of 5 to 30° at an angle of 2θ, while the XRPD of quench-cooled CAR revealed a halo effect similar to that of amorphous silica.

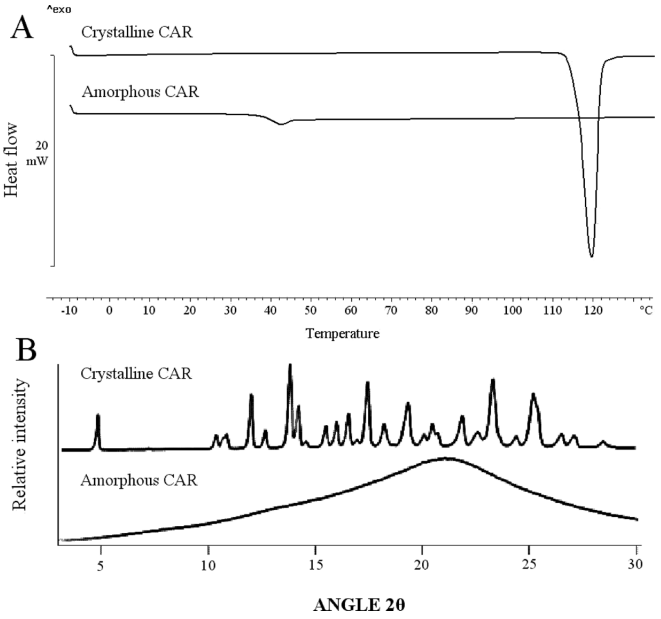

Fig. 1. DSC Curves (A) and XRPD Spectra (B) of Crystalline and Quench-Cooled (Amorphous) CAR

The median particle size of crystalline CAR was 41.5 μm, and the size of crushed amorphous CAR ranged from 100 to 150 μm. By grinding the amorphous CAR in a cool environment, particles of 39.3 μm average diameter were obtained. Grinding did not cause crystallization. Figure 2A displays a SEM image of amorphous CAR and Fig. 2B shows C6 solid dispersion particles. Measured median particle size of Sylysia and C6 solid dispersion particles was in range from 8 to 10 μm, and the shape of solid dispersion particles was similar to Sylysia particles. No isolated particles of CAR can be seen within the solid dispersion, which suggests that CAR is well dispersed within the carrier's particles.

Crystalline State of CAR in SD The XRPD patterns of the samples in Fig. 3 showed that the level of crystallinity decreased with decreasing amounts of CAR in the SD. C1 shows no sharp diffraction lines, which means that no crystalline CAR was present on the surface or in the silica pores. Samples C2 and C4 show diffraction lines at angles that correspond to those of crystalline CAR. It is assumed that the CAR-rich samples contained more CAR than could be accommodated within the pores of silica and that CAR in those cases was in a partially crystalline state. The DSC curves of SDs from set A experiments (Fig. 4) confirm the higher content of crystalline CAR in the SD with higher drug load. Beside glass transition, two distinctive melting peaks were observed in samples C4 and C6. The more evident peak, at the higher temperature, conformed to the melting temperature of CAR polymorph II. The XRPD spectra of C4 (Fig. 3) showed the same characteristic diffraction lines as pure CAR polymorph II (Fig. 1) and there was no evidence of another polymorph form present. Additional thermogravimetric analysis (data not included) confirmed that no water or other solvent had been adsorbed onto sample particles. The possible explanation for a lower melting temperature is the melting point depression which is most evident in nanoparticles.[40] The two melting peaks of the DSC curve can be therefore attributed to the crystallization of CAR inside pores

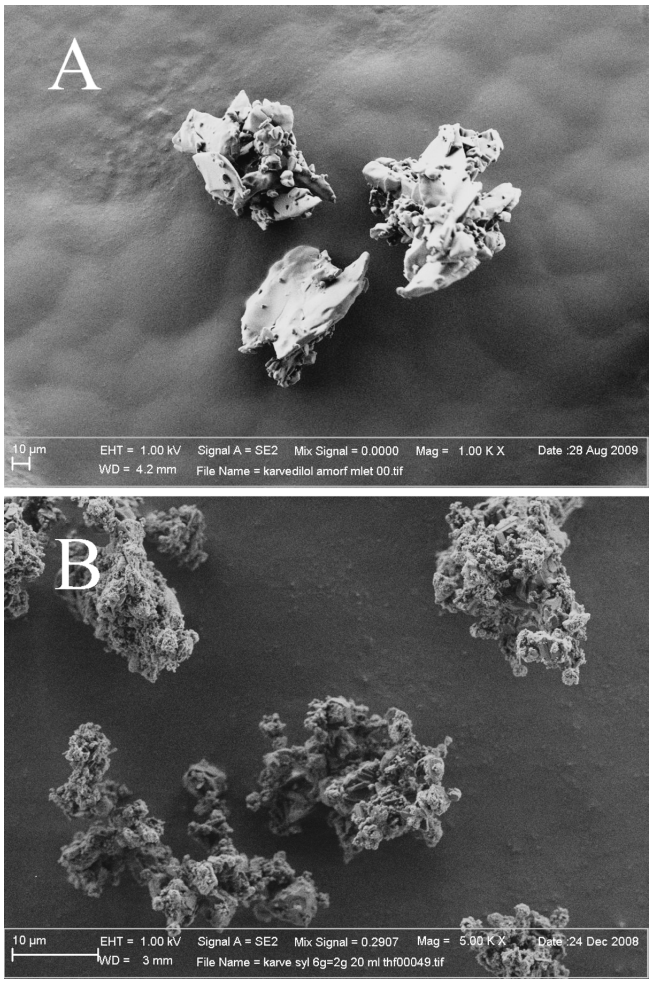

Fig. 2. SEM Images of (A) Amorphous CAR (Mag. 1000×), (B) C6 SD Particles (Mag. 5000×)

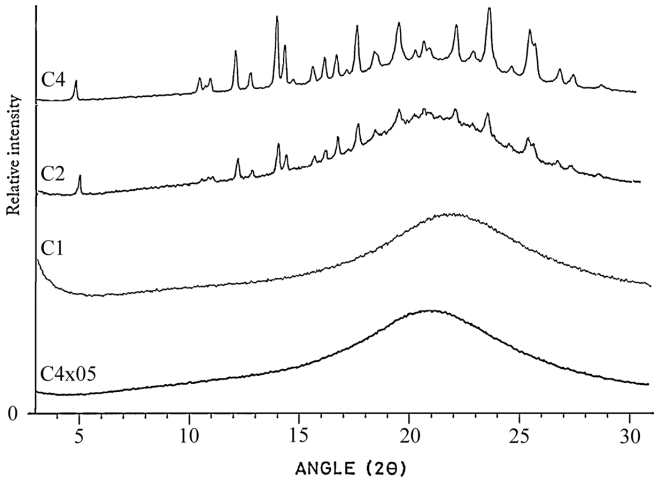

Fig. 3. The XRPD Spectra of SD Set A Particles Containing Different Amounts of CAR (C4, C2, C1) and SD of Set B Particles (C4×05) (See Table 1 for the Composition of Individual Samples)

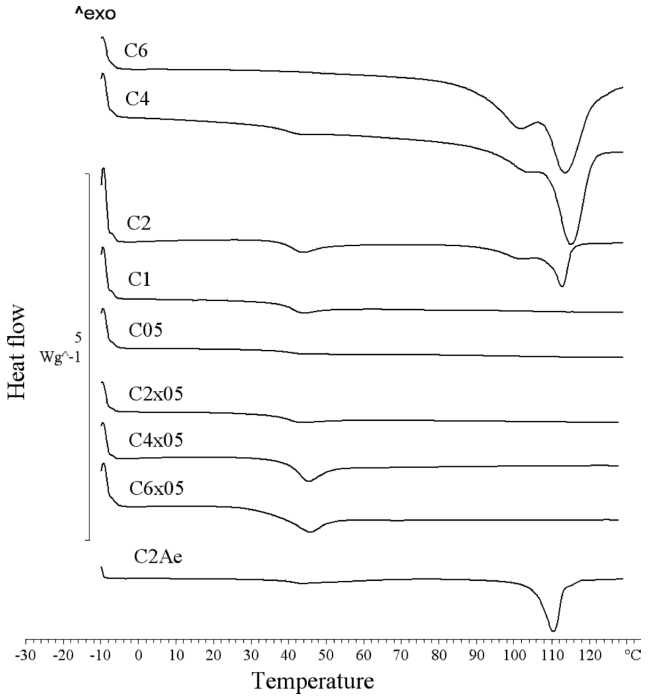

Fig. 4. DSC Curves of Set A (C6, C4, C2, C1, C05), Set B (C2×05, C4×05, C6×05) and C2Ae SDs

and on the exterior silica surfaces during preparation of solid dispersions. The absence of a melting peak and notable T_g at 38 °C, for SDs with a lower CAR content indicated that the CAR is amorphous in these solid dispersions. It can be concluded from these data that the content of CAR in a SD prepared by the one-step filling process should be 33 w/w% or less in order to assure a completely amorphous drug state in the SD.

On DSC curves of SDs from set B experiments (Fig. 4) no melting peaks were observed and the T_g values were proved that CAR is completely amorphous in all samples, even in sample C6×05, where the CAR content in the SD was 60%. This indicates that CAR was deposited onto the silica surface in a different manner, ensuring precipitation and stabilization of the amorphous phase in higher quantities compared to set A SDs.

Adsorption and Deposition of CAR onto the Silica Carrier The tendencies of CAR adsorption onto the silica surface, regardless of material porosity, were determined using adsorption studies. Liquid dispersions of dissolved CAR and dispersed Aerosil 200 were prepared. Aerosil 200 was chosen for the adsorption studies due to its defined nonporous surface and the fact that its chemical composition is the same as Sylysia 350. Even though 2.0 g (4.9 mmol) of dissolved CAR was dispersed in suspensions using varying amounts of Aerosil 200, we could not detect a decrease in the level of dissolved CAR in the THF solution, a quality that would be otherwise attributed to an adsorption onto the solid's surface. It is known that the adsorbability of molecules onto the surface of dispersed silica is strongly dependant on the polarity and electron-donating properties of a solvent, which influence the interaction of a drug with a solvent. In general, when the energy of the drug interaction with the solvent is dominant, the adsorption level onto the carrier's surface is low.[41] The same results were obtained for adsorption studies using porous Sylysia 350. This confirms that the silica surface itself does not interact with dissolved CAR in a THF solution.

The effect of the silica's porosity on CAR's solid-state properties was examined by preparing a SD with Aerosil 200, using the same drug-to-carrier ratio as the C2 sample (2.0 g : 2.0 g). This sample is denoted as C2Ae. On DSC thermogram of C2Ae (Fig. 4) evident melting peak is noted. A small portion of amorphous CAR, which is evident from slight T_g on DSC curve, can be attributed to deposition of CAR inside small number of pores within aggregated Aerosil 200 particles during preparation of SD. It can be concluded that drug precipitation inside the porous matrix creates amorphous CAR, while drug precipitation on the pores' exterior surfaces creates crystalline CAR.

In a recent study, Godec *et al.* examined how the pore size of porous materials within which a compound is entrapped influences the crystal structure of the precipitated compound and what the critical pore size would be that would prevent crystallization of the compound from the solution or the amorphous solid state.[42] The minimum size of a nucleus formed from the solution can be calculated and, once the compound is entrapped in pores of a smaller size than the minimum size of a nucleus, it cannot crystallize. They agree that the amorphous state may be stable even within spaces larger than those predicted by their equations, taking into account other possible effects such as adsorption of the amorphous form onto pore walls, hydrogen bonding between silica and the investigated compound, and so on. Each possible effect would contribute to stabilization of the amorphous compound.[41] Sylysia 350 has a nominal average pore diameter of 25 nm. Using gas adsorption analysis, it was confirmed that about 29 m^2/g of Sylysia's surface (10% of the total surface area) area is located within pores of a diameter below 5 nm and at the same time that 29 m^2/g of the surface area is located in pores of diameter above 44 nm. It is therefore reasonable to assume that some of the drug precipitates deeper into the porous matrix in the region of smaller pores and other portions remain in the region of wider pores. The final effect of this drug distribution inside the porous matrix is shown as crystalline CAR.

The results of wetting analysis, specific surface area, average pore diameter, and average pore volume of samples are summarized in Table 2. Wetting properties of the powder samples are represented as the value of initial contact angle of dissolution media on the surface of powder plates and as the rate of imbibition of dissolution media drop (2 μl) into the sample. Increased contact angles are consistent with the increased drug concentrations in the dispersion and reflect increment of surface hydrophobicity. The contact angle for sample C6×05 is not consistent with drug load. The possible reason for measured value of contact angle could be the preparation of the sample, where some handling was required for preparation. Additionally, in most cases the liquid drop formed on the powder plates was not static. For this reason also imbition rate was measured. It was impossible to measure contact angle and imbibition rate of the liquid with pure Sylysia because of highly porous and hydrophillic properties which caused immediate suction of a drop after its deposition on a powder plate. It could be claimed that for investigated samples imbibition rate of dissolution media drop is a better indicator of powder sample's hidrophilicity than initial contact angle measurement. These values are in good correlation with the drug load, specific surface area and average pore volume.

Table 2. Wetting Properties, Specific Surface Area, and Porosity of Samples

Sample	Contact angle, rate of imbibition	Specific surface area (m^2/g)	Average pore diameter (nm)/ average pore volume (cm^3/g)
CAR	75°, no imbib.	—	—
CAR amorphous	72°, no imbib.	—	—
Sylysia 350	—	277.5	25.3/1.75
C05	44°, 0.170 μl/s	185.8	27.4/1.26
C1	51°, 0.040 μl/s	127.9	27.4/0.86
C2	51°, 0.013 μl/s	79.8	28.6/0.56
C4	60°, no imbib.	48.5	26.8/0.32
C6	63°, no imbib.	28.7	25.9/0.18
C2×05	59°, 0.025 μl/s	126.6	28.1/0.88
C4×05	59°, 0.007 μl/s	61.6	30.1/0.46
C6×05	51°, no imbib.	19.0	34.4/0.16

It is noteworthy that with increasing CAR content in the SD particles of set A, values of specific surface area and average pore volume decreased, but average pore-diameter values and distribution of pore size did not. In all samples of set A particles 10% of total surface area is located within pores of a diameter below 5.0—5.6 nm and at the same time 10% of total surface area is located within pores of a diameter above 39—42 nm. It can be assumed that some of the drug precipitated inside these mesopores and thus entirely filled them. This should theoretically result in an increase of pore diameter. However, some of the drug also adsorbed onto the walls of the wider pores and decreased their diameter which is in correlation with decreased wettability of the solid dispersions with aqueous media. Independently from the drug concentration in solid dispersion particles both types of drug deposition resulted in constant average pore diameter and similar pore size distribution in comparison to pure Sylysia 350.

The result was different with set B samples, where the average pore diameter widened from 25 to 34 nm in SD particles as CAR content increased. Also, the porosity of SD particles was more sharply reduced as CAR content increased in set B particles compared with set A particles. This resulted in a much slower rate of dissolution media imbibition when comparing C20 and C4×05 samples that contained same amount of CAR (50%). N_2 adsorption analysis showed that 10% of total surface area is located within pores of a diameter below 5.6, 4.0 and 2.7 nm in samples C2×05, C4×05 and C6×05, respectively, while 10% of total surface area is located within pores of a diameter above 38, 53 and 92 nm in samples C2×05, C4×05 and C6×05, respectively. It could be concluded that in these samples more CAR precipitated in form of particles that can also occlude pores of the carrier and less of the drug adsorbed onto the walls in comparison to set A dispersions.

Stability of CAR in SD Particles Amorphous CAR and SD samples C1, C2 and C6×05 were stored for 12 months at room temperature, open to ambient moisture. At time zero, CAR in the SD was completely amorphous or only a slight portion was in the crystalline state (Fig. 4). Figure 5 shows the DSC and TGA curves of the amorphous CAR after 12 months. The shape of DSC curve indicates an exothermic recrystallization event at temperatures between 60 °C and

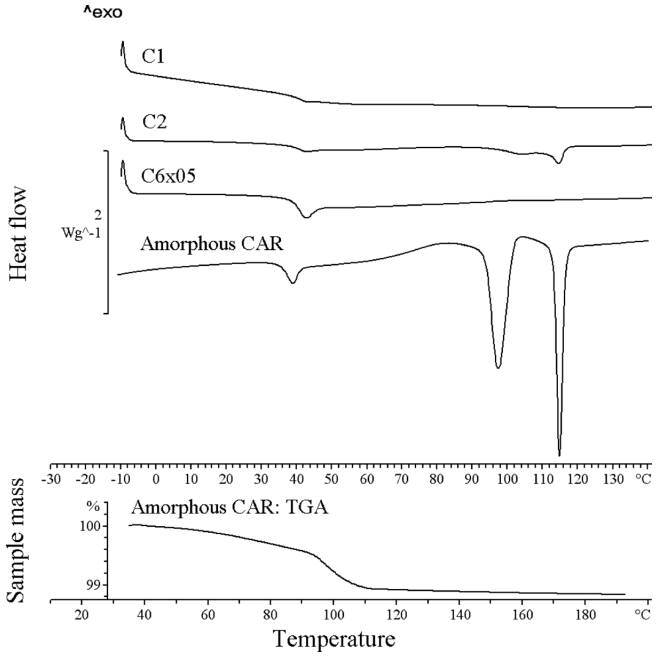

Fig. 5. DSC Curves of C1, C2, C6×05 and Amorphous CAR (TGA Curve Included) after 12 Months

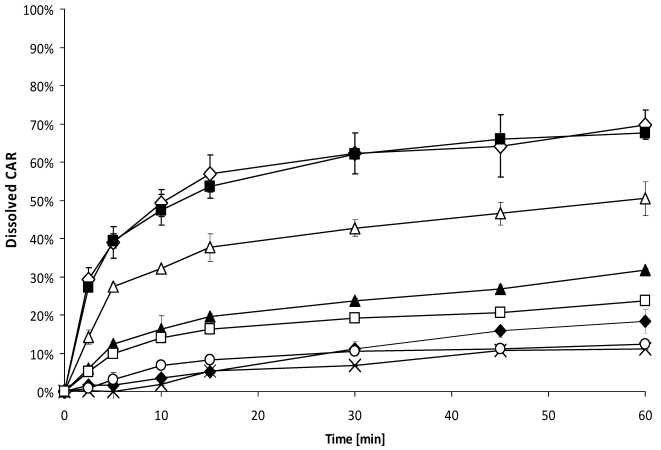

Fig. 6. Dissolution Profiles of CAR from SD Particles with Sylysia 350: (◆) CAR Crystals, (×) CAR Amorphous, (▲) C2, (◇) C05, (○) C6, (■) C2×05, (△) C4×05, (□) C6×05

90 °C with following melting point at onset temperature of 95 °C. This is in accordance to described preparation and properties of stable polymorph modification III of CAR.[43,44] According to the experiments disclosed in the cited literature, polymorph III could be prepared by crystallization from water or precipitation from organic solvent by addition of water used as anti-solvent. During aging period amorphous CAR adsorbed a significant amount of moisture (1.1%), which is evident from loss of mass at temperature close to 100 °C and confirmed with mass spectrometry analysis. After melting of polymorph III recrystallization of polymorph II occurs. Additional XRPD studies confirmed the presence of polymorph III at ambient temperature and the presence of polymorph II at 110 °C.

Figure 5 shows also the DSC curves of selected SD samples after 12 months. The CAR in sample C1 remained amorphous, although it is apparent from the shape of the DSC curve that some moisture was absorbed into the hydrophilic porous carrier. In sample C2, the portion of crystallized CAR had slightly increased. Remarkably, the DSC curve of C6×05 had remained identical to that at the beginning which indicated resistance to moisture sorption and good stability of the amorphous CAR in SD particles.

Dissolution Property of CAR in SD Particles The dissolution profiles of SDs containing CAR are summarized in Fig. 6. The experiment was not carried out under sink conditions and the drug was not completely dissolved in 1 h, but under conditions such that the dissolution study was most discriminatory and in our opinion biologically relevant.

Crystalline CAR exhibited a faster dissolution rate in comparison to the pure amorphous drug. About 20% of the crystalline CAR was dissolved, while only 10% of the amorphous drug was dissolved over the same period. Pokharkar *et al.*[17] described and explained this phenomenon using CAR's low T_g value (38 °C), which is essentially the same as the temperature of the dissolution medium and might have caused it to convert from amorphous CAR into a cohesive super-cooled liquid state. During the dissolution process of amorphous CAR, the un-dissolved substance remained in a non-crystalline state.

The differences in the dissolution behavior of SDs were generated within the first 15 min and strongly correlated with the drug-to-silica ratio (CAR content). After the initial burst dissolution, which determined the overall dissolution performance, CAR then slowly and linearly dissolved throughout the remaining time, independent of sample type. The most extensive burst dissolution was observed in samples with the lowest CAR content in the SD: C05 and C2×05 (20% and 33% CAR, respectively). Samples C2 and C4×05 (both 50% CAR) exhibited different dissolution rates, with C4×05 being faster. The slowest rates were for C6 and C6×05 (75% and 60% CAR, respectively), which dissolve slower than pure crystalline CAR and at about the same rate as pure amorphous CAR.

There were several factors governing dissolution kinetics. As seen from a comparison of wetting properties and dissolution profiles, those factors may be the amount of amorphous/crystalline CAR in the SD, porosity, and hydrophilicity of particles. By analogy with the dissolution properties of amorphous CAR, a greater amount of amorphous CAR should extend the release. In this case, however, the level of amorphicity was indicative of more effective drug loading inside the pores, which caused a greater amount of the drug to be finely dispersed along the silica surface and a more intense interaction of CAR with the silanol groups. This lessened drug agglomeration and improved its apparent wettability. That CAR was finely dispersed along silica's surface at lower concentration (C05 and C2×05) is reflected also in relatively high specific surface area and porosity of these dispersions. Good wettability of these SDs and dissolution pressure, as described by Kelvin's equation for particles of size below 1 μm,[45] increase solubility and dissolution rate to the greatest extent. When dissolution medum entered the porous matrix, it began to completely saturate highly hydrophilic silanol surfaces, and it competitively displaced hydrophobic molecules from the hydrophilic carrier's surface. At that point, CAR was dislodged from the carrier's particles into the dissolution medium, so the distribution of CAR molecules

inside the porous matrix played an important role in determining the initial dissolution rate. As the drug content in SD increases also imbibition of the dissolution medium into pores decreases which results in slower release of CAR. CAR-rich SDs evidently had more hydrophobic surface area and reduced porosity because of intense packing, which negatively affected the wetting of particles. Water molecules were deflected from the carrier's surface and the capillary rise of the dissolution medium with a subsequent displacement of drug particles inside the porous matrix did not take place. Under these circumstances, the drug was slowly released from particles *via* surface erosion.

Conclusion

Solid dispersion particles of CAR with porous silica (Sylysia 350) were prepared by the solvent method using a THF solution and two different pore-filling procedures. It was found that the crystallinity, amorphicity, and dissolution behavior of CAR can be controlled using various drug content levels and methods of SD preparation. Samples with lower CAR content showed remarkable improvement in terms of the dissolution rate of CAR from SD particles. Preparation of SDs with porous silica using a multiple-step pore-filling procedure allowed for high content levels of the amorphous drug, which then remained physically stable over a period of 12 months under ambient conditions. One-step pore-filling method of CAR did not result in high content levels of the amorphous drug in SD. Specific surface area and porosity parameters, along with the measured wetting properties of SD samples, confirmed different mechanism of drug loading within silica pores and suggested their influence on CAR's crystalline state, physical stability, and dissolution properties.

Acknowledgments The authors would like to thank Krka d. d., Novo mesto for supporting the study. This research was partly financed by the European Union's European Social Fund.

References and Notes

1) Stegemann S., Leveiller F., Franchi D., De Jong H., Lindén H., *Eur. J. Pharm. Sci.*, **31**, 249—261 (2007).
2) Löbenberg R., Amidon G. L., *Eur. J. Pharm. Biopharm.*, **50**, 3—12 (2000).
3) Morgan T., *Clin. Pharmacokinet.*, **26**, 335—346 (1994).
4) Wei L., Sun P., Nie S., Pan W., *Drug Dev. Ind. Pharm.*, **31**, 785—794 (2005).
5) Noyes A. A., Whitney W. R., *J. Am. Chem. Soc.*, **19**, 930—934 (1897).
6) Chaumeil J. C., *Methods Find. Exp. Clin. Pharmacol.*, **20**, 211—215 (1998).
7) Wen X., Tan F., Jing Z., Liu Z., *J. Pharm. Biomed. Anal.*, **34**, 517—523 (2004).
8) Bhutani S., Hiremath S. N., Swamy P. V., Raju S. A., *J. Sci. Ind. Res.*, **66**, 830—834 (2007).
9) Hirlekar R., Kadam V., *J. Incl. Macrocycl. Chem.*, **63**, 219—224 (2009).
10) Hancock B. C., Parks M., *Pharm. Res.*, **17**, 397—404 (2000).
11) Fukuoka E., Makita M., Yamamura S., *Chem. Pharm. Bull.*, **35**, 2943—2948 (1987).
12) Datta S., Grant D. J. W., *Nat. Rev. Drug Discov.*, **3**, 42—57 (2004).
13) Andronis V., Yoshioka M., Zografi G., *J. Pharm. Sci.*, **86**, 346—351 (1997).
14) Yu L., *Adv. Drug Deliver. Rev.*, **48**, 27—42 (2001).
15) Simonelli A. P., Metha S. C., Higuchi W. I., *J. Pharm. Sci.*, **58**, 538—549 (1969).
16) Chiou W. L., Riegelman S., *J. Pharm. Sci.*, **58**, 1505—1509 (1969).
17) Pokharkar V. B., Mandpe L. P., Padamwar M. N., Ambike A. A., Mahadik K. R., Paradkar A., *Powder Technol.*, **167**, 20—25 (2006).
18) Monkhouse D. C., Lach J. L., *J. Pharm. Sci.*, **61**, 1435—1441 (1972).
19) Rupprecht H., Biersack M. J., Kindl B., *Colloid Polym. Sci.*, **252**, 415—416 (1974).
20) Vrečer F., "PhD Thesis," University of Ljubljana, Slovenia, 1992.
21) Takeuchi H., Nagira S., Yamamoto H., Kawashima Y., *Powder Technol.*, **141**, 187—195 (2004).
22) Takeuchi H., Nagira S., Yamamoto H., Kawashima Y., *Int. J. Pharm.*, **293**, 155—164 (2005).
23) Uchino T., Yasuno N., Yanagihara Y., Suzuki H., *Pharmazie*, **62**, 599—603 (2007).
24) IUCLID Data set for the European Commission, Silicon Dioxide, 2000.
25) "Seventeenth Report of the Joint FAO/WHO Expert Committee on Food Additives," Wld. Hlth. Org. techn. Rep. Ser., 1974, No. 539; FAO Nutrition Meetings Report Series, No. 53, 1974.
26) Sylysia FCP, Product Information, Fuji Sylisia Chemical Ltd., Aichi, Japan.
27) Takeuchi H., Nagira S., Tanimura S., Yamamoto H., Kawashima.Y., *Chem. Pharm. Bull.*, **53**, 487—491 (2005).
28) Brinker C. J., "Colloidal Silica: Fundamentals and Applications," ed. by Bergna H. E., Roberts W. O.,Taylor and Francis, New York, 2005, pp. 615—633.
29) Ahola M., Kortesuo P., Kangasiniemi I., Kiesvaara J., Yli-Urpo A., *Int. J. Pharm.*, **195**, 219—227 (2000).
30) Chen J., Ding H., Wang J., Shao L., *Biomaterials*, **25**, 723—727 (2004).
31) Ohta K. M., Fuji M., Takei T., Chikazawa M., *Eur. J. Pharm. Sci.*, **26**, 87—96 (2005).
32) Otsuka M., Tokumitsu K., Matsuda Y., *J. Controlled Release*, **67**, 369—384 (2000).
33) The International Conference on Harmonisation of Technical Requirements for Registration of Pharmaceuticals for Human Use (ICH). "Topic Q3C (R4) Impurities: Guideline for Residual Solvents." <http://private.ich.org/LOB/media/MEDIA5254.pdf>, cited 15 October, 2010.
34) Brunauer S., Emmett P. H., Teller E., *J. Am. Chem. Soc.*, **60**, 309—319 (1938).
35) Lippens B. C., De Boer J. H., *J. Catal.*, **4**, 319—323 (1938).
36) Barrett E. P., Joyner L. G., Halenda P. P., *J. Am. Chem. Soc.*, **73**, 373—380 (1951).
37) Starov V. M., *Adv. Colloid Interface Sci.*, **111**, 3—27 (2004).
38) Chen W. M., Zeng L. M., Yu K. B., Xu J. H., *Chin. J. Struct. Chem.*, **17**, 325—328 (1998).
39) Beyer P., Reinholz E., European Patent Application 0,893,440 (1999).
40) Couchman P. R., Jesser W. A., *Nature* (London), **269**, 481 (1977).
41) Pogorelyi V. K., Barvinchenko V. N., Pakhlov E. M., Smirnova O. V., *Coll. J.*, **67**, 172—176 (2005).
42) Godec A., Maver U., Bele M., Planinšek O., Srcic S., Gaberscek M., Jamnik J., *Int. J. Pharm.*, **343**, 131—140 (2007).
43) Hildesheim J., Finogueev S., Aronhime J., Dolitzky B., Ben-Valid S., Kor I., PCT Publication WO 02/00216 (2002).
44) Chen W., Gallop M., Oh C., PCT Publication WO 03/005970 (2003).
45) Müller R. H., Böhm B. H. L., Grau M. J., "Handbook of Pharmaceutical Controlled Release Technology," 1st ed., ed. by Wise D. L., Marcel Dekker, New York, 2000, pp. 345—357.